www.serd.ait.ac.th/reric

Analysis of Heat Pipe Solar Collector with different Heat Pipe Parameter

B. Sivaraman*[1] and N. Krishna Mohan*

Abstract- *Heat Pipe Solar Collector (here after referred as HPSC) has better collecting efficiency compared to the conventional collector, besides overcoming some of the drawbacks encountered with the later one. In this paper, numerical simulation & theoretical analyses of HPSC parameters are presented. The effects of L_c/L_e (Condenser length /Evaporator length) ratio and L/d_i (length/diameter) ratio of heat pipe on HPSC were analysed. Simulated results were compared with experimental values. Heat pipes (Five numbers each) having two different L_e/L_c, with two different L/d_i have been designed, fabricated, and used in the solar collector absorber. Copper and Stainless steel have been used as container and wick material of heat pipe and Methanol has been used as working fluid. Heat pipes are designed to have heat transport factor of around 194 W and 260 W of thermal energy. The experiments were conducted during summer season with a collector tilt angle of 11^o &13^o to the horizontal. It was found experimentally that the collector with less L/d_i ratio was more efficient. This improved efficiency is due to increase in heat transport factor of heat pipe, which increases with decrease in L/d_i ratio. Numerical simulation also shows that when the L/d_i increases, the efficiency of the collector decreases. Similarly the performance of HPSC was found to be better with higher L_c/L_e value. The numerical simulation also has the same trend.*

Keywords - Heat pipe, capillary limit, solar collector, wick, numerical simulation.

1. INTRODUCTION

The use of heat pipes in the field of solar energy has proved fruitful and solar water heater is one among the various applications of it. The thermal diode property, control over the temperature and efficient heat transfer capability of heat pipe can be effectively utilized by suitable design. Heat pipe in solar absorbers has many advantages over conventional collectors (instantaneous efficiency, 25-30%). It has superior heat conduction, thermal diode benefit and it responds quickly to any changes in radiation intensity. The major shortcomings of conventional solar collector are the liquid reverse motion during night and freezing of liquid in the tube during cold conditions. Such drawbacks can be overcome by replacing transport pipe with a heat pipe [1] - [19]. Bienert and Wolf [4] first reported the use of heat pipe in solar collectors. Soin et al[17], [18] investigated the performance of solar collector with fluid undergoing phase change and reported the effect of insolation and the liquid level on the collector performance of a thermosyphon collector containing acetone and petroleum ether. Akyurt [12] designed and tested the heat pipes on prototype solar water heater and found that heat pipes perform satisfactorily as heat transfer elements. Schreyer [14] reported that there was six percent increase in instantaneous efficiency, due to the use of refrigerant R-11 in a thermosyphon collector. Nesreen and Yvonne [13] fabricated and tested R-11 charged solar collector with an integrated condenser for secondary cooling water flow.

Hussein et al [9] investigated theoretically and experimentally the transient thermal behaviour of a wickless heat pipe flat plate solar collector. Kamminga [11] investigated theoretically the performance of an evacuated tubular collector with heat pipe using Fourier frequency domain. Al-Hindi et al [3] developed an intermittent duty solar refrigerator assisted by heat pipes. Hammad [8] studied the performance of flat plate solar collector cooled by a set of heat pipes. Jorge Facao [10] analysed hybrid solar collector (plate type heat pipe) using artificial neural network, reported that the ANN is an efficient, and time saving technique. Soteris et al [19] modeled solar water heating system using ANN.

This paper presents the numerical simulation of HPSC. The parameters that were considered in the analysis are L/d_i, L_c/L_e, water inlet temperature, collector tilt angle and solar intensity, where L, L_c, L_e and d_i are total length, condenser length, evaporator length and inner diameter of heat pipe respectively.

2. DESCRIPTION OF THE SYSTEM

Design of Heat Pipes

Heat pipe is a very simple and efficient heat transfer device for transferring heat from a source to a sink by means of evaporation and condensation of a fluid in a sealed system. This sealed unit has a working fluid which absorbs the heat energy from the evaporator and transfers it to the condenser. The capillary action of wicks returns the condensate to the evaporator. The outstanding feature of heat pipe is its ability to accept heat non-uniformly (considerable change in the heat flux input may not affect the performance of the heat pipe). Heat pipes of 1 m total length with two different internal diameters and two different L_c/L_e ratios were designed, fabricated, and used in the solar collector (Table 1) to study their effect on the performance of HPSC. Two sets of heat pipe (each set of five numbers) with copper pipe of 1 m total length; evaporator and condenser length of 0.85 m & 0.15 m

*Mechanical Engineering, Annamalai University, Annamalainagar, Tamilnadu India 608 002

[1]Corresponding Author:
Tel: 00914144 239733; E-mail: siv_gee@rediffmail.com

respectively having two different internal diameter of 17 mm and 19 mm were designed, fabricated and used in the HPSC to study the effect of L/d_i ratio. To analyse the L_c/L_e effect, another two sets of heat pipe (each set of five numbers) with internal diameter of 17 mm having two different evaporator and condenser length of 0.75, 0.85 m & 0.25, 0.15 m respectively were designed and fabricated. The maximum capillary limit (the heat load on heat pipe due to maximum capillary pressure for liquid wick combination) of the heat pipes were 194.25 W and 268.48 W. The designed heat transfer limit is sufficient to transfer the heat intercepted and gained by the absorber plate of the solar collector, as the maximum heat gained by the plate was around 300 W only. Such heat pipes (5 Numbers) were used in the solar collector and placed over the absorber plate (Fig.1). Wrapped screen wick structure with two layers of wick was used in the heat pipe (Fig.2).

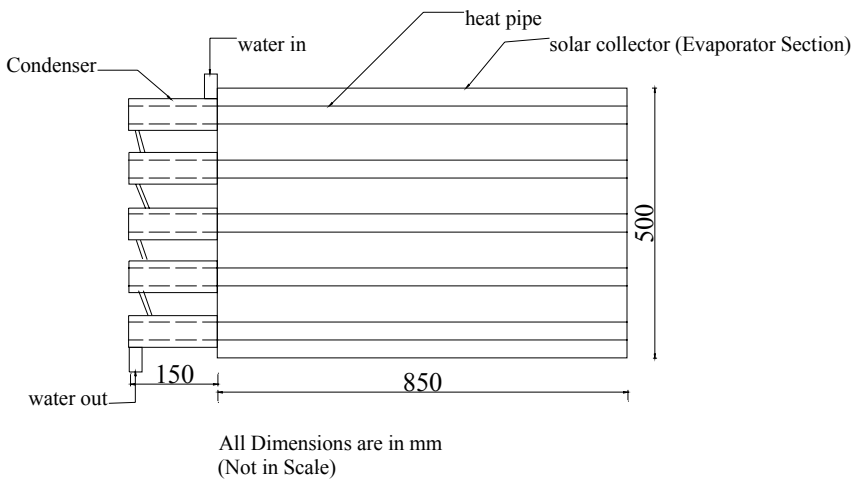

Fig. 1. Top view of the collector.

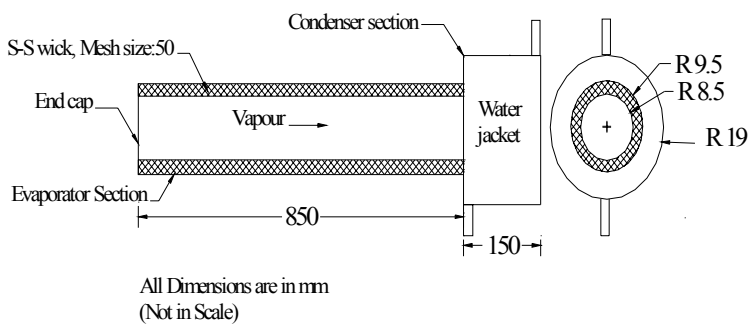

Fig. 2. Details of heat pipe.

Design of Solar Collector

Solar collector is a flat plate collector (0.85 m x 0.5 m) with single glass covering. The collector absorber is a 2 mm thick black painted aluminum sheet. The heat pipes (5 Nos evenly spaced over the collector) were mounted on to the absorber sheet in such a way that the evaporator section of the heat pipe is within the collector and the condenser section is protruding outside the collector. The sides and back of the collector were properly insulated. All the five condenser sections of the heat pipes have been connected serially. The collector was placed facing directly south with different tilt angles to the horizontal, to study its effect on HPSC. Copper – Constantan thermocouples were provided in the collector to measure the temperatures of absorber plate, glass plate and surface of the heat pipe at two different locations on each heat pipe in the evaporator section, one being nearer to the condenser section.

Table 1. Specifications of Heat pipes

Description	Pipe – 1	Pipe – 2	Pipe – 3	Pipe – 4
Outer diameter of the heat pipe, m	0.019	0.022	0.019	0.019
Inner diameter of the heat pipe, m	0.017	0.019	0.017	0.017
Total length, m	1.0	1.0	1.0	1.0
Evaporator length, m	0.85	0.85	0.85	0.75
Condenser length, m	0.15	0.15	0.15	0.25
Wick mesh size number	50	50	50	50
Capillary limit, W	194.25	268.48	194.25	194.25
Sonic limit, W	52578.78	62392.93	52578.78	52578.78
Entrainment limit, W	2070.21	2800.4	2070.21	2070.21
Boiling limit, W	1784.81	1158.8	1784.81	1574.832

Experimental Setup

Experiments were conducted with the designed HPSC for two different mass flow rates (0.0033 & 0.0083 kg/s) on various days and observations were recorded every 20 min (10.00 A.M - 4.00 P.M). Solar intensity at the test site (Location: Annamalainagar, Latitude: 11^o N) was measured using EPPLY pyranometer. The water inlet and exit temperatures were measured using mercury in glass thermometer. The flow rate was measured using graduated rotameter.

3. NUMERICAL SIMULATION OF HEAT PIPE SOLAR COLLECTOR

This section presents the detailed theoretical analysis of the heat pipe solar collector. The performance of the collector was studied by the numerical simulation procedure. The simulation procedure involves casting governing mathematical equations for each system components by balancing the energy into and out of it and then combining these models consecutively to accomplish complete simulation of the system. The heat pipe solar collector system components are glass cover, absorber plate, evaporator, wick, working fluid, condenser, circulating water and heat exchanger. The individual components governing equations were then non-dimensionalized and the resultant equation was written as finite difference equation form using Crank-Nicolson

method. The system of simultaneous equation was then solved.

System component modelling

A schematic sketch of the heat pipe solar collector under study is shown in Fig. 3. For the thermal analysis of the collector, the following assumptions were made to simplify the problem.

1. The entire system is in thermal equilibrium with the ambient.
2. Glass cover temperature is assumed uniform at any given instant.
3. The temperature gradient across the absorber plate thickness and across the thickness of the heat pipe wall may be neglected.
4. The temperature gradient in the longitudinal direction in the evaporator section can be neglected, since the evaporator section of heat pipe is subjected to constant solar energy
5. The sides of the collector are well insulated, hence the edge losses are neglected in the analysis.
6. The bond resistance between the absorber and heat pipe are neglected.
7. Vapour temperature inside the heat pipe is that of saturation temperature.

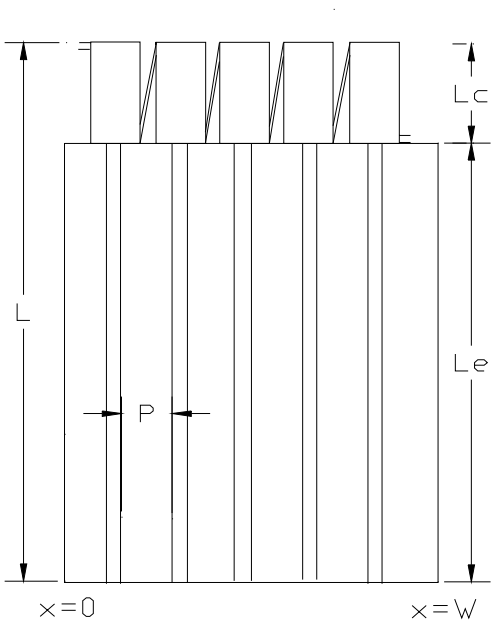

Fig. 3. Schematic of HPSC.

The glass cover governing equation can be written in the dimensional form (W/m^2)

$$\rho_g \delta_g C_g \frac{dT_g}{dt} = \alpha_g I_t + U_{pg}\left(T_p - T_g\right) - h_{cga}\left(T_g - T_a\right) - h_{rga}\left(T_g - T_\alpha\right) \tag{1}$$

where

U_{pg} is the overall heat loss coefficient between the absorber plate and glass cover.

h_{cga} & h_{rga} are the convective and radiation heat transfer coefficient between glass cover and ambient.

The absorber plate governing equation per unit area is given by (W/m^2)

$$\rho_p \delta_p C_p \frac{\partial T_p}{\partial t} = k_p \delta_p \frac{\partial^2 T_p}{\partial x^2} + \langle \tau_g \alpha_p \rangle I_t - U_{pg}\left(T_p - T_g\right) - U_b\left(T_p - T_a\right) \tag{2}$$

Subject to the boundary conditions given

$$\frac{dT_p}{dx} = 0 \quad \text{at} \quad x = 0 \,\&\, w, \quad t \geq 0 \tag{3}$$

$$T_p = T_e \quad \text{at} \quad x = x \quad t \geq 0 \tag{4}$$

where

I_t, the global solar radiation is theoretically estimated using Lingamgunta &Veziroglu [6] correlation

U_b is the bottom loss coefficient of the collector.

The energy balance equation of the evaporator section is given by (W/m)

$$\rho_e A_{ecs} C_e \frac{\partial T_e}{\partial t} = \langle \tau_g \alpha_p \rangle I_t d_o - k_p \delta_p \left(\frac{\partial T_p}{\partial x}\right)_x - \frac{\pi d_o}{2} U_{eg}\left(T_e - T_g\right) - \pi d_v h_e \left(T_e - T_s\right) - k_{eff} L_e \frac{T_e - T_{wk}}{\delta_{wk}} - \frac{\pi d_o}{2} U_b \left(T_e - T_a\right) \tag{5}$$

where k_{eff} is the effective thermal conductivity of the wick structure.

The heat transfer coefficient of evaporator is given by

$$h_e = \frac{4}{3}\left[\frac{\rho_l^2 k^3 g h_{fg}}{4\mu_l \left(T_e - T_s\right) L_e}\right]^{\frac{1}{4}} \tag{6}$$

The working fluid inside the heat pipe is fully saturated and its energy balance equation is given by (W)

$$\frac{\pi d_v^2}{4} \rho_l V_t^* L_t C_l \frac{dT_s}{dt} = \pi d_v L_e h_e \left(T_e - T_s\right) - \pi d_v L_c h_c \left(T_s - T_c\right) \tag{7}$$

The energy balance of the heat pipe wick is given by (W/m^3)

$$\left(\rho C\right)_{eff} \frac{\partial T_{wk}}{\partial t} = k_{eff} \frac{\partial^2 T_{wk}}{\partial y^2} \tag{8}$$

where $\left(\rho C\right)_{eff} = \varphi\left(\rho C\right)_l + \left(1 - \varphi\right)\left(\rho C\right)_{wk}$ φ is the porosity of the wick. Since the wick is liquid saturated, the wick temperature can be taken as in thermal equilibrium with saturation temperature of the liquid.

The energy balance of a differential element of a condenser section of heat pipe solar collector is given by (W/m)

$$\rho_c A_{ccs} C_c \frac{\partial T_c}{\partial t} = k_c A_{ccs} \frac{\partial^2 T_c}{\partial y^2} + \pi d_v h_c \left(T_s - T_c\right) + k_{eff} L_c \left(\frac{T_{wk} - T_c}{\delta_{wk}}\right) - \pi d_o h_{fi} \left(T_c - T_w\right) \tag{9}$$

subject to the boundary conditions

$$T_c = T_s \quad at \quad y = 0, \quad t \geq 0 \tag{10}$$

$$\frac{dT_c}{dy} = 0 \quad at \quad y = L_c, \quad t \geq 0 \tag{11}$$

The heat transfer coefficient of condenser is given by

$$h_c = \frac{4}{3}\left[\frac{\rho_l^2 k^3 g h_{fg}}{4\mu_l \left(T_s - T_c\right) L_c}\right]^{\frac{1}{4}} \tag{12}$$

h_{fi} is the convective heat transfer coefficient of water flowing inside the heat exchanger.

The energy balance of the differential element of water inside the heat exchanger is given by (W/m)

$$\rho_w A_w C_w \frac{\partial T_w}{\partial t} + \dot{m}_w C_w \frac{\partial T_w}{\partial y} = \pi d_o h_{fi} \left(T_c - T_w\right) - \pi d_1 h_{fo} \left(T_w - T_{ex}\right) \quad (13)$$

with the boundary condition

$$T_w = T_{wi} \quad at \quad y = 0, \quad t \geq 0 \quad (14)$$

h_{fo} is the outer convective heat transfer coefficient of the heat exchanger.

The energy balance of the differential element of a heat exchanger is given by (W/m)

$$\rho_{ex} A_{excs} C_{ex} \frac{\partial T_{ex}}{\partial t} = k_{ex} A_{excs} \frac{\partial^2 T_{ex}}{\partial y^2} + \pi d_1 h_{fo} \left(T_w - T_{ex}\right) - \pi d_2 U_{ex} \left(T_{ex} - T_a\right) \quad (15)$$

with the following boundary conditions

$$\frac{dT_{ex}}{dy} = 0 \quad at \quad y = 0 \,\&\, L_c \quad t \geq 0 \quad (16)$$

The above governing equation of components and boundary conditions are converted into non-dimensional form to generalize the analysis by defining dimensionless parameters for coordinates, temperature, radiation and time as

$$X = \frac{x}{w} \quad Y = \frac{y}{L_c} \quad \theta = \frac{k_p \left(T - T_a\right)}{I_{sc} P} \quad \tau = \frac{k_p t}{\rho_p C_p P^2} \quad (17)$$

$$I_T = \frac{I_t}{I_{sc}}$$

where I_{sc} is the solar constant.

The non-dimensionalised governing equations are then written in finite difference form using Crank-Nicolson scheme for the partial differential equations and by modified Euler's scheme for the ordinary differential equations. The absorber plate, condenser section of heat pipe, the circulating water and heat exchanger are discretized and solved.

The simulation procedure

The numerical procedure for solving the above set of finite difference equations is as follows:

The initial temperatures of all the components of the collector were set.

Non-dimensional time step of 0.001 was set for the simulation of collector performance.

The starting time and ending time of simulation were set.

Given the collector tilt angle, day of the year, collector configuration, cooling water inlet temperature, ambient temperature the simulation of the collector performance commences.

The output of the simulation was saved after each iteration and the output data were used for the theoretical analysis of the collector performance.

4. RESULTS AND DISCUSSION

Experimental results

Water was used as cooling fluid in the condenser of heat pipe. Figure.4 shows the instantaneous efficiency curve of the HPSC system for a day. A maximum collector efficiency of around 67 % was obtained during peak sunshine hour and the fluid outlet temperature of 318 K, while the fluid inlet temperature was kept at 308 K. Figure.5 shows the plot of efficiency curve for different L/d_i ratio of heat pipe. It is very clear from the plot when the L/d_i is reduced the performance of the collector improves.

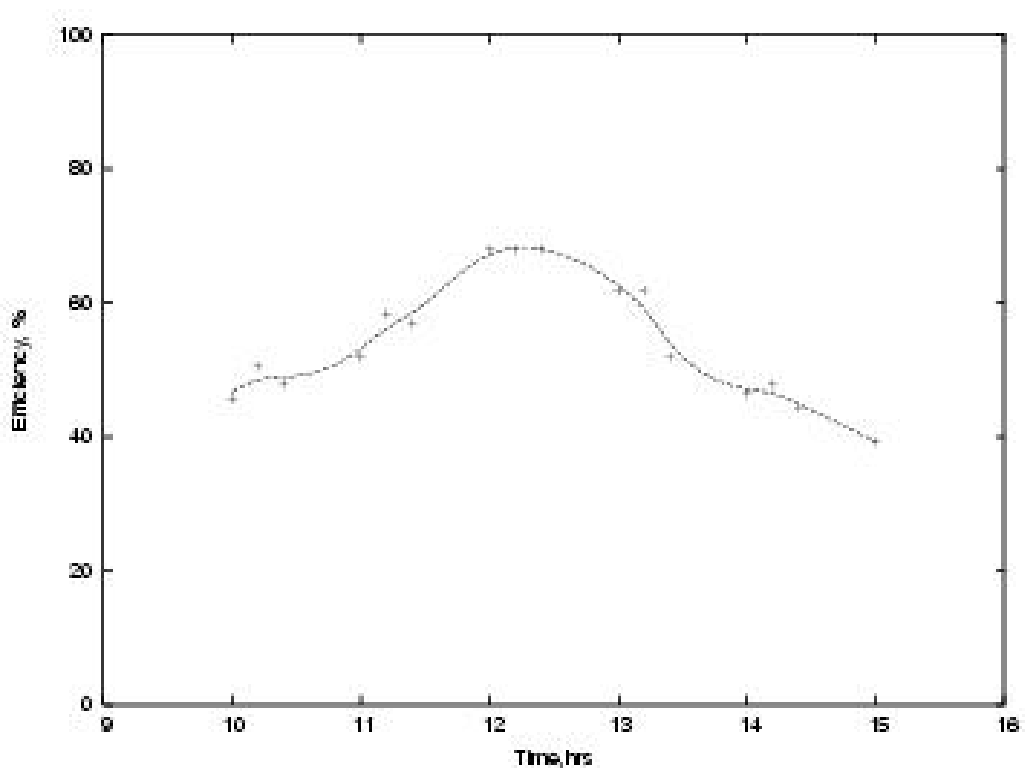

Fig. 4. Efficiency vs. Time.

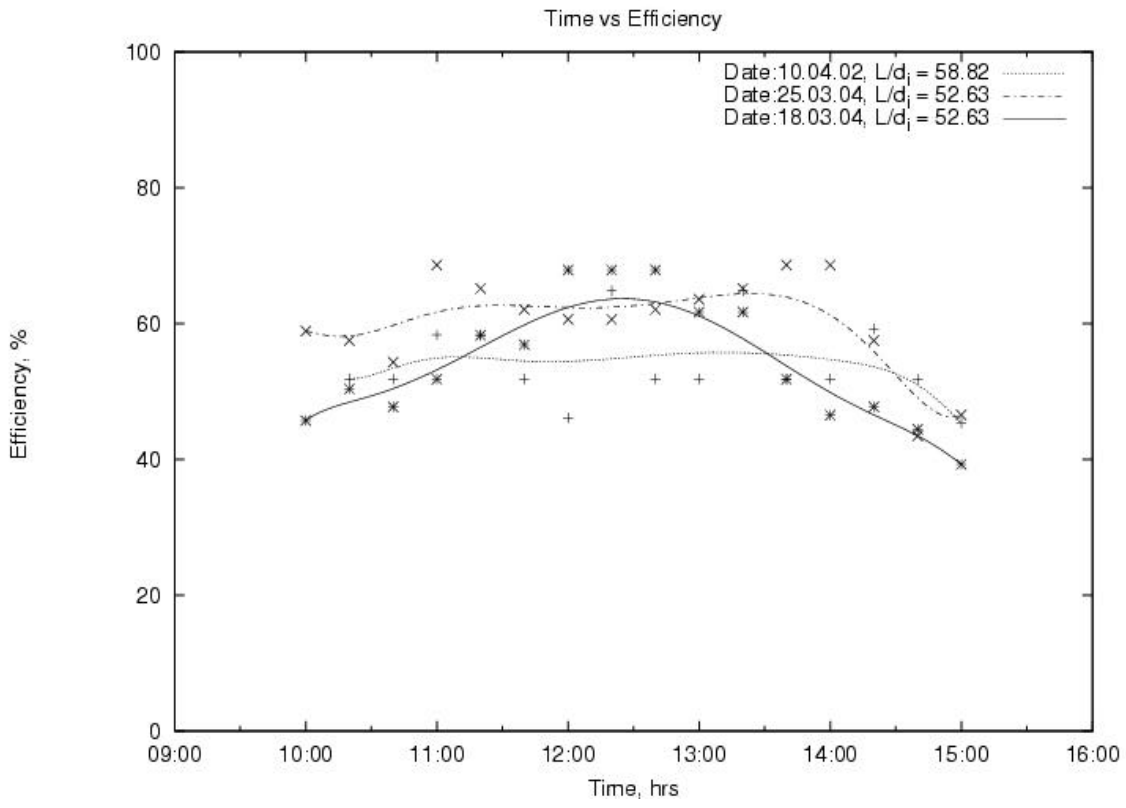

Fig. 5. Efficiency vs. Time for different L/d$_i$ ratio.

In Fig. 5, the efficiency curve for the day 25.03.04 shows the lesser performance, since the condenser end of the heat pipe was kept at bottom, in which case the working fluid had to be transported only by capillary action of the wick. Figure. 6 confirms that the working fluid flow is hampered by the position of the condenser. When the condenser section is kept at below the evaporator the temperature build up on the evaporator side is more due to slow transport of fluid to that section and hence the evaporation rate is less , ultimately resulted in poor performance of the collector system as it is shown in Figs. 7 & 8. From Fig. 8 it is also evident that the rise in temperature of water goes down as flow rate increases. Figure. 9 show the plot of time vs. water outlet temperature of the collector for different flow rates of cooling water on the collector side. The curve is in good agreement that when flow rate increases the rise in water temperature decreases. Figure 10 shows the variation of water outlet temperature with different L_c/L_e ratio, When that ratio was increased, the performance was good since the condensation rate got improved resulting in more quantity of working fluid flow to the evaporator at any given instant consequently increases the evaporation rate.

Numerical results

The set of governing equations of the system components of HPSC were simultaneously solved using the procedure given earlier and the temperature of individual components were obtained. Figure 11 compares the experimental and numerical prediction of water outlet temperature of the collector. The predicted results were in good agreement with the experimental values. The percentage error of the predicted value is less than ± 5 percent at any given time. The error may be due to round off and truncation error of numerical method adopted and also due to instrumentation error of experimental data. The numerical results are within the allowable error limit.

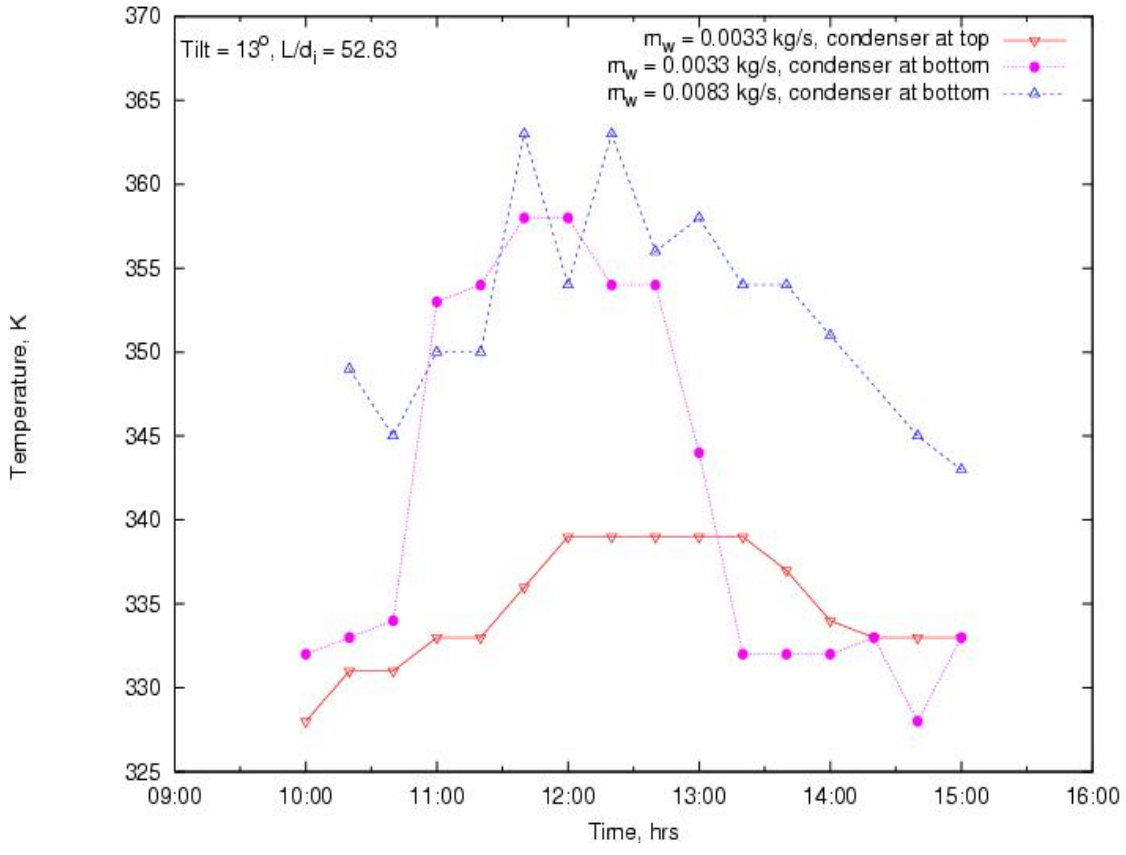

Fig. 6. Time vs. Evaporator temperature for different condenser position.

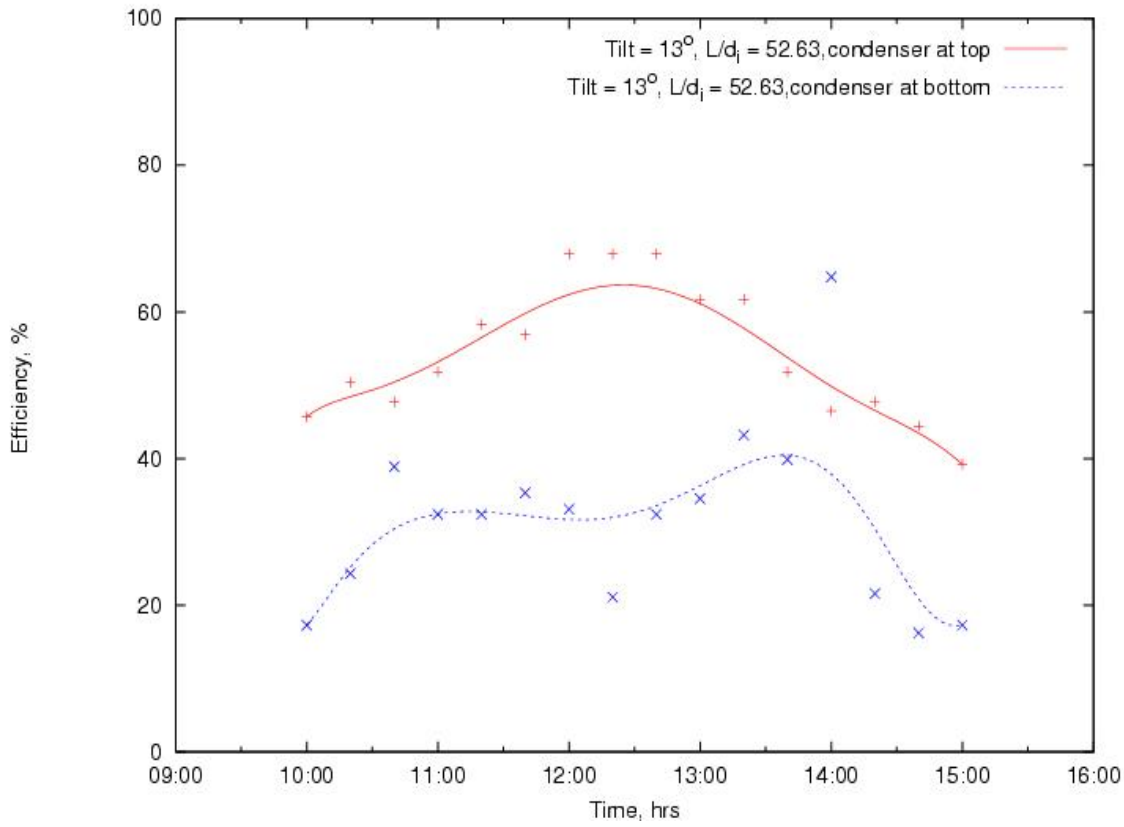

Fig. 7. Time vs. Efficiency with different L/d$_i$ ratio.

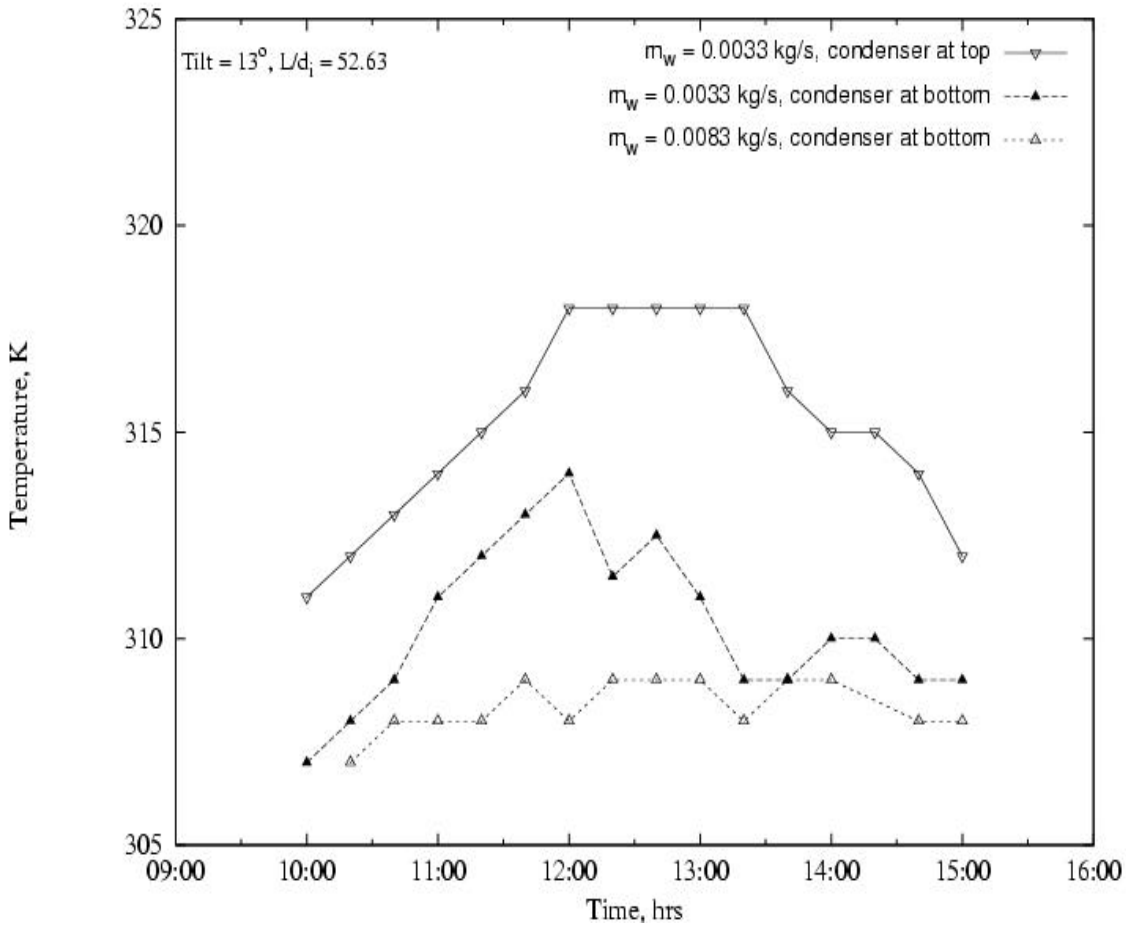

Fig. 8. Time vs. Water outlet temperature for different flow rate & L/d$_i$ ratio.

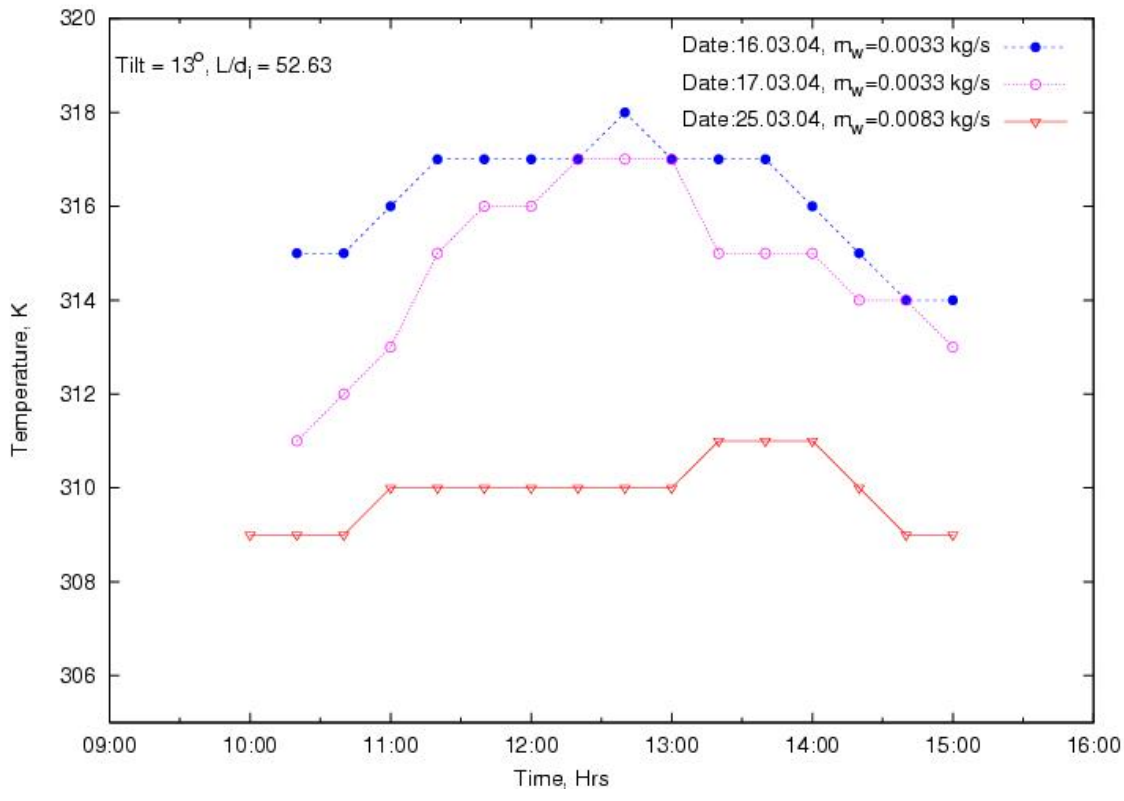

Fig. 9. Water outlet temperature vs. Time for different flow rate.

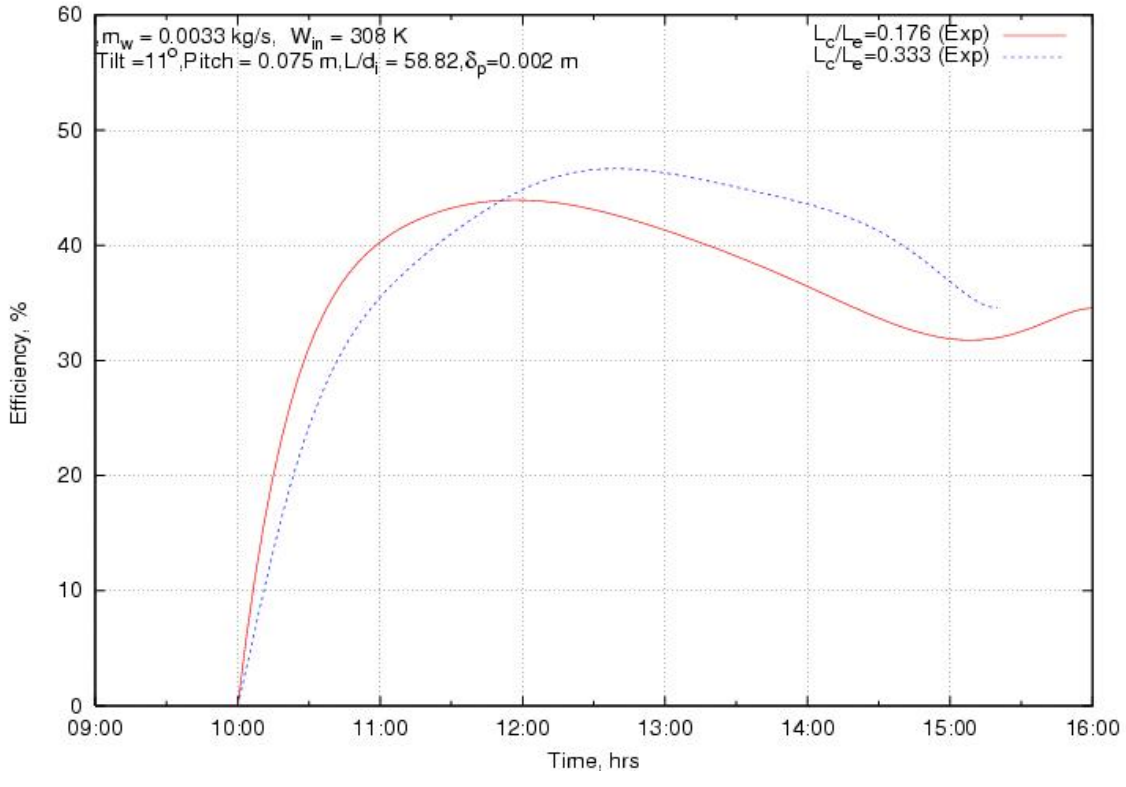

Fig. 10. Water outlet temperature vs. Time for different L_c/L_e ratio.

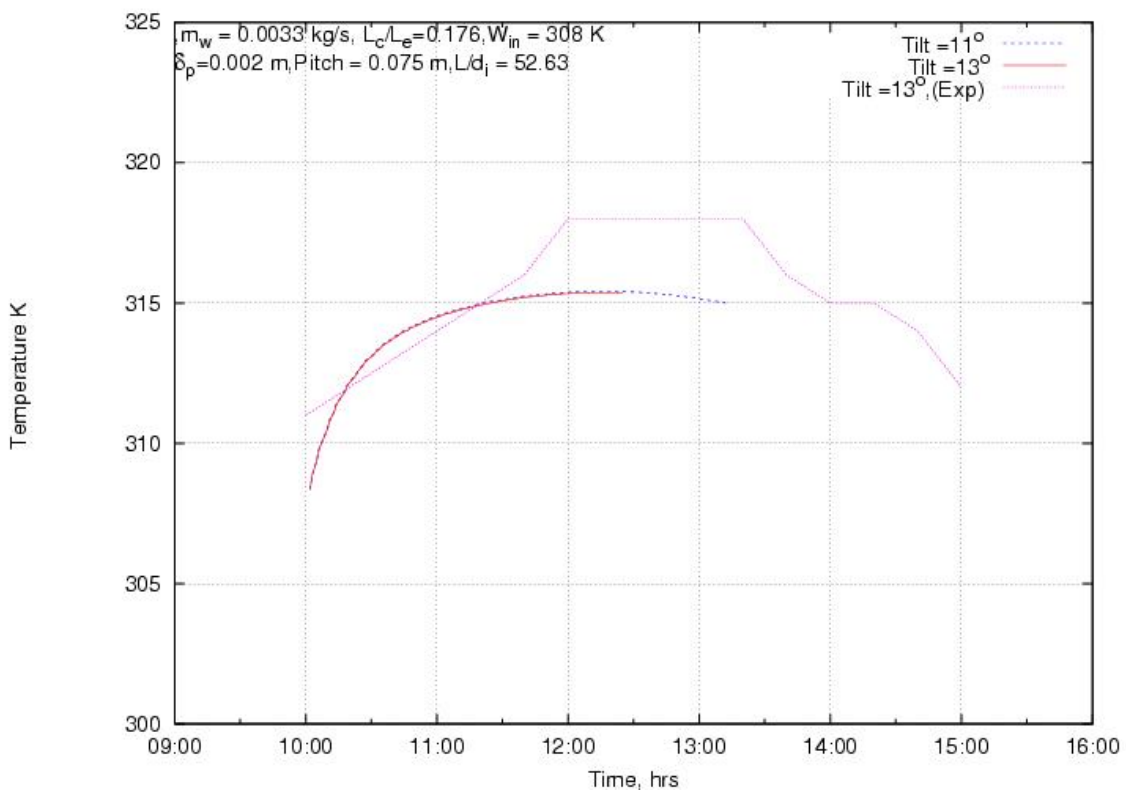

Fig. 11. Experimental & Numerical result of $T_{w_{out}}$.

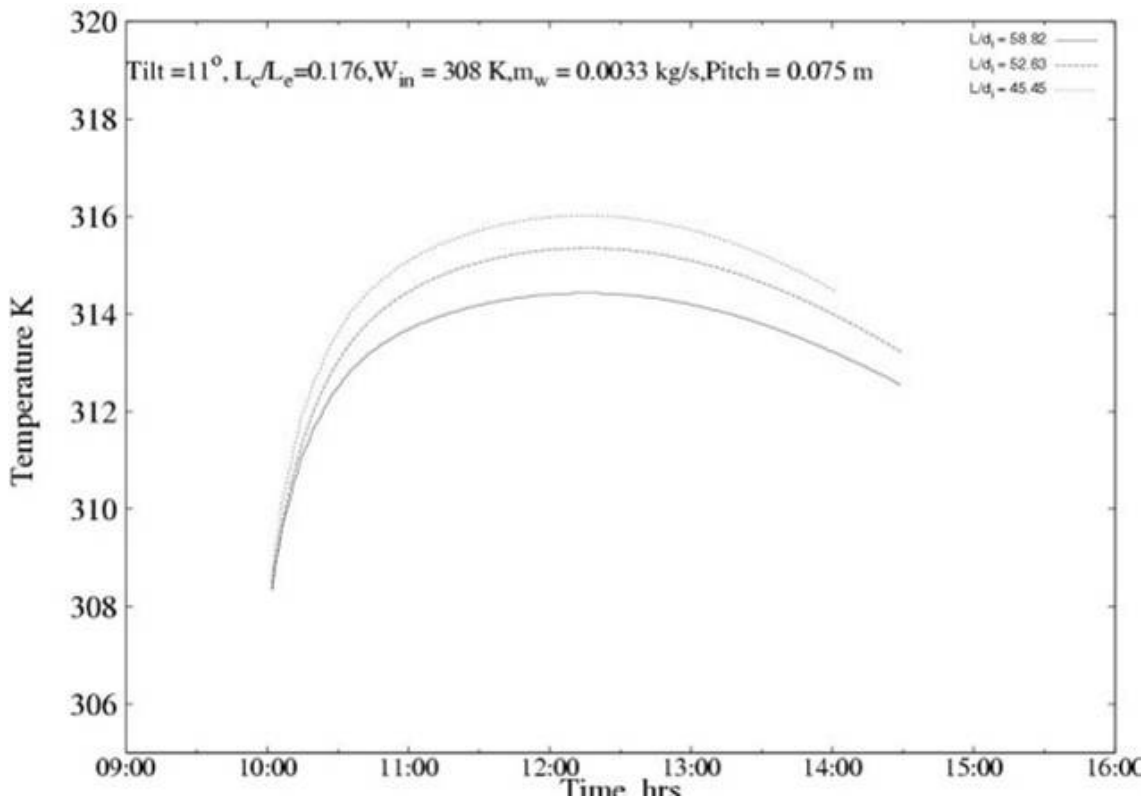

Fig. 12. Effect of L/d_i ratio on collector performance.

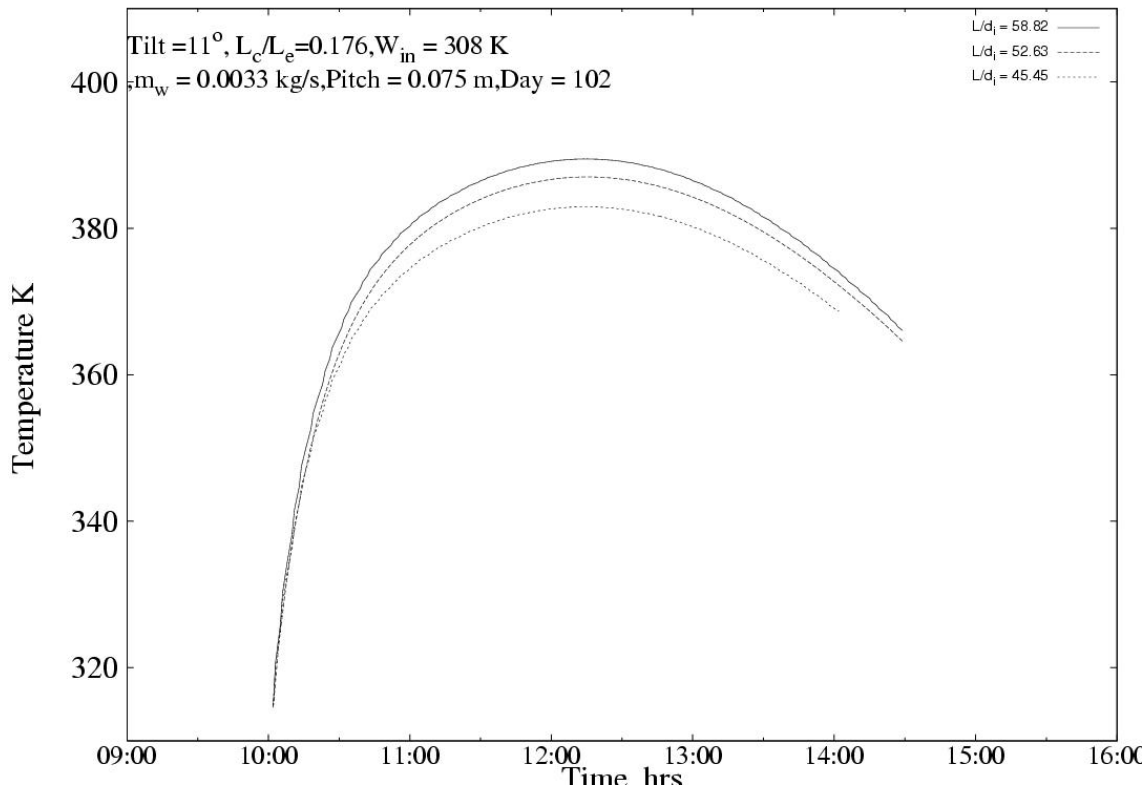

Fig. 13. Effect of L/d_i ratio on Evaporator wall temperature.

Figures 12 & 13 shows the effect of L/d_i ratio of heat pipe on the output water temperature and on one of the evaporator wall temperature of the HPSC for the similar conditions of other parameters. With decrease in L/d_i ratio, the water outlet temperature increases, where as the evaporator wall temperature decreases as expected which is due to accumulation of heat on the evaporator side due to less condensation rate on the condenser side of the heat pipe. Figure 14 shows the same effect of this ratio on the performance of collector when the L_c/L_e ratio was changed. Figure 15 shows that same trend is obtained when the absorber plate thickness was changed. The effect of L_c/L_e ratio of heat pipe on the outlet temperature of HPSC is plotted in Fig. 16, which show that the predicted results are following the trend as expected. Though that variation is nil during the initial hours of exposure to sunlight, there exists a gradient as time passes and again the gradient decreases when the solar flux falls down. The variation of temperature is minimal, but 5 to 8 % increase in the instantaneous efficiency of the collector will be obtained for the same.

Figures. 17 & 18 show the effect of thickness of absorber plate (δ_p) on the water outlet temperature of the HPSC. The heat gained by the absorber with 2 mm thick is more during initial hours of exposure, but the response of 3 mm thick absorber overtake at later stage. The mass flow rate effect on the performance of the HPSC is plotted in Fig. 19. The trend of the curve shows the same trend as reported for the experimental work. The effect of heat pipe working fluid on the HPSC is reported in Figs. 20 & 21. The simulation was carried out for three working fluids namely for methanol, Acetone and water. Almost same performance was predicted for acetone and methanol. The heat exchanger dimensional parameter's effect was shown in Fig. 22. The increase in the internal diameter of heat exchanger results in decrease in the outlet temperature of water. This may be due to increase in overall heat transfer coefficient of heat exchanger as a result of which more heat is transferred to the ambient.

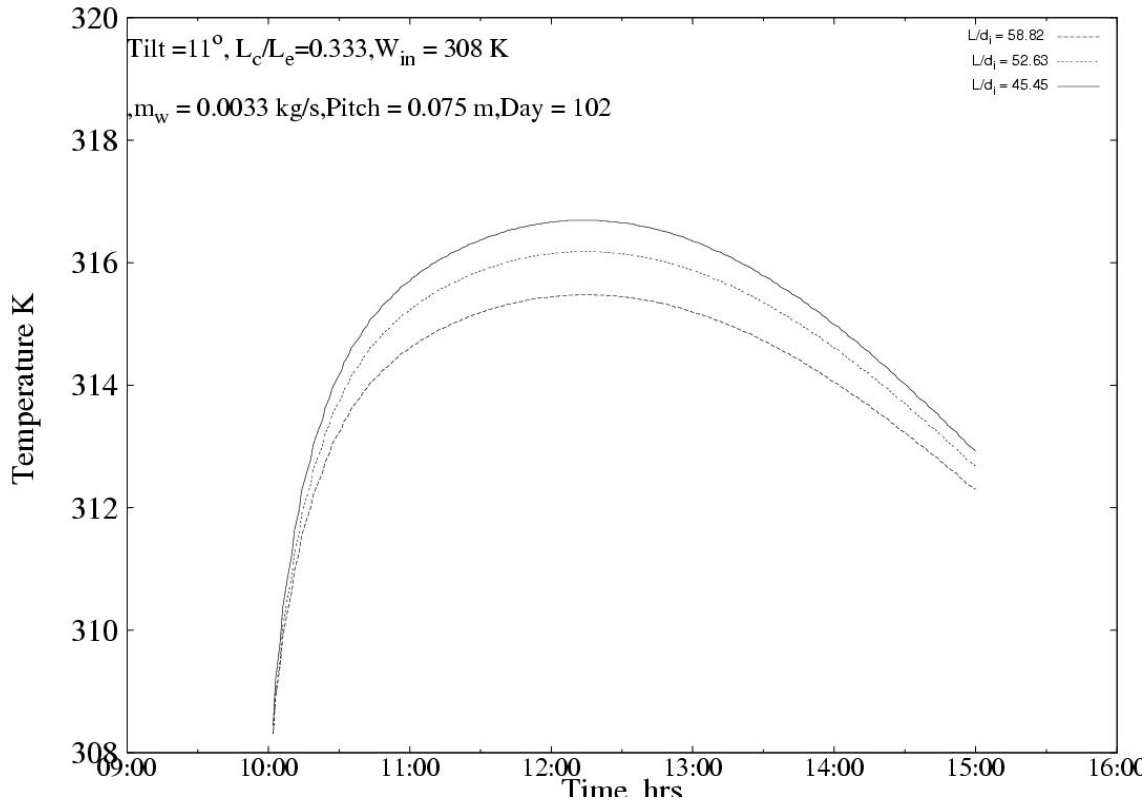

Fig. 14. Effect of L/d_i ratio on $T_{w_{out}}$.

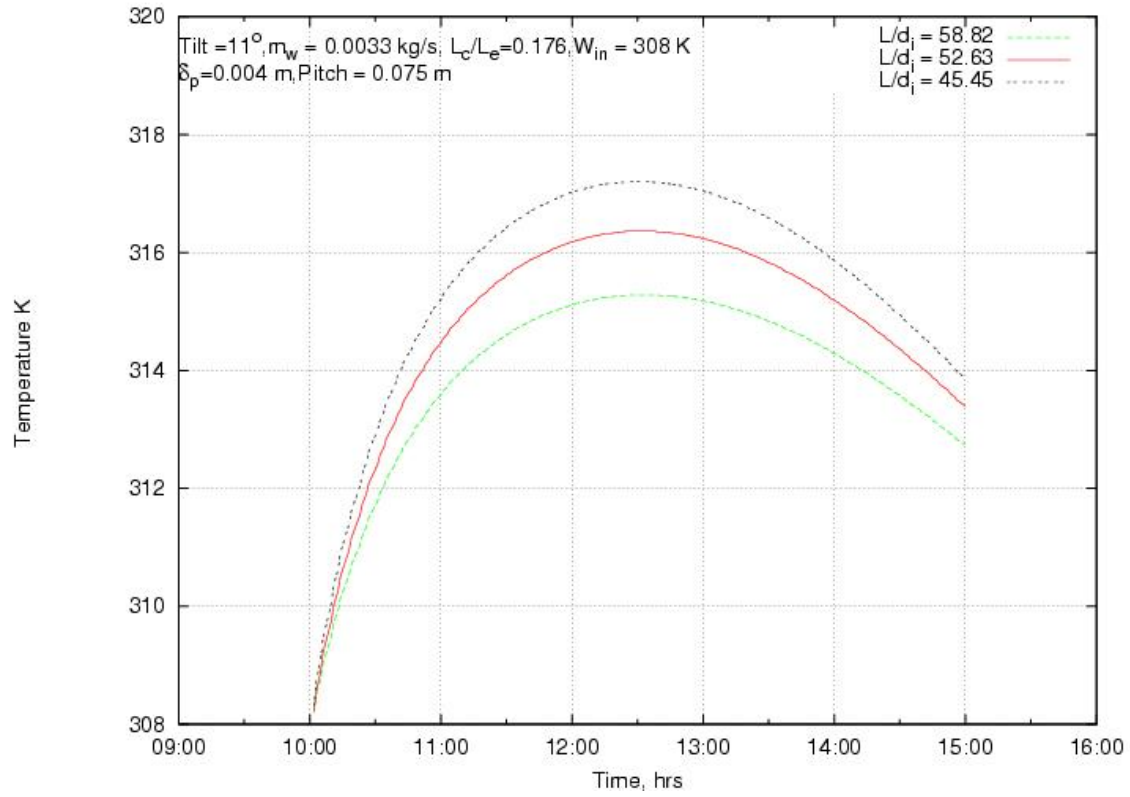

Fig. 15. Effect of L/d_i ratio on $T_{w_{out}}$.

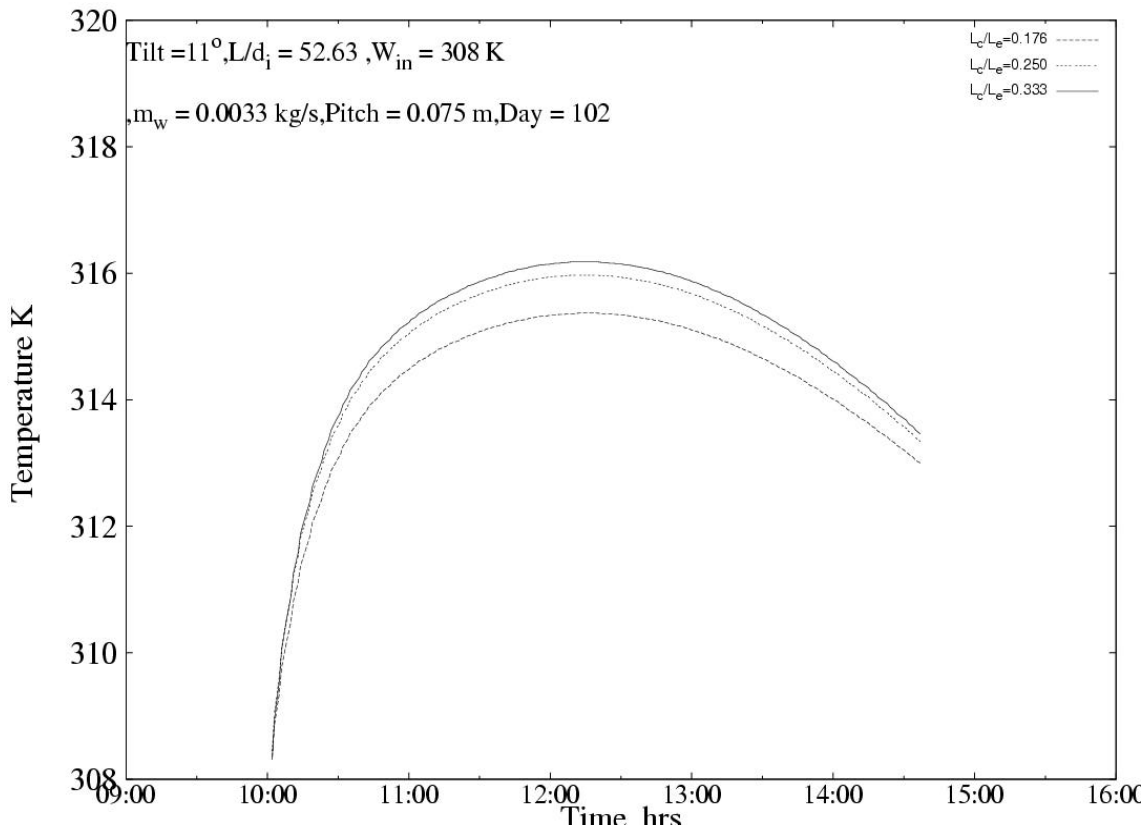

Fig. 16. Effect of L_c/L_e ratio on $T_{w_{out}}$.

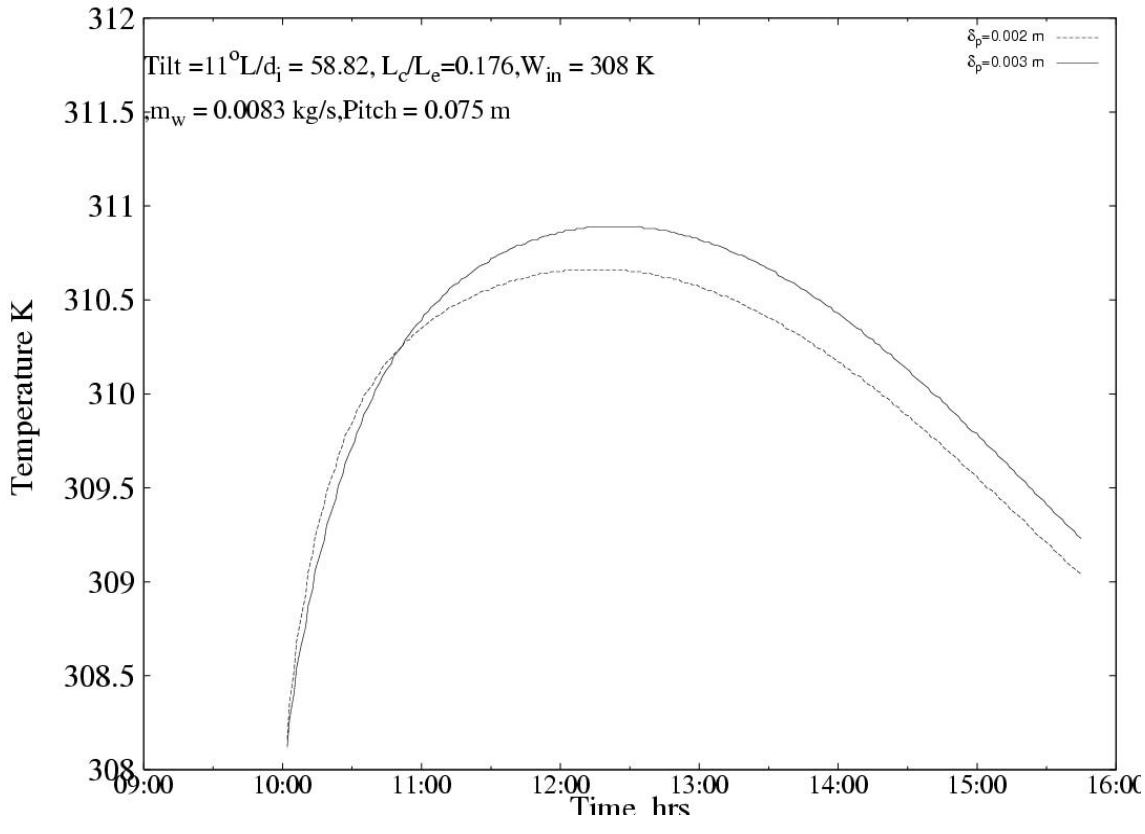

Fig. 17. Effect of δ_p on $T_{w_{out}}$.

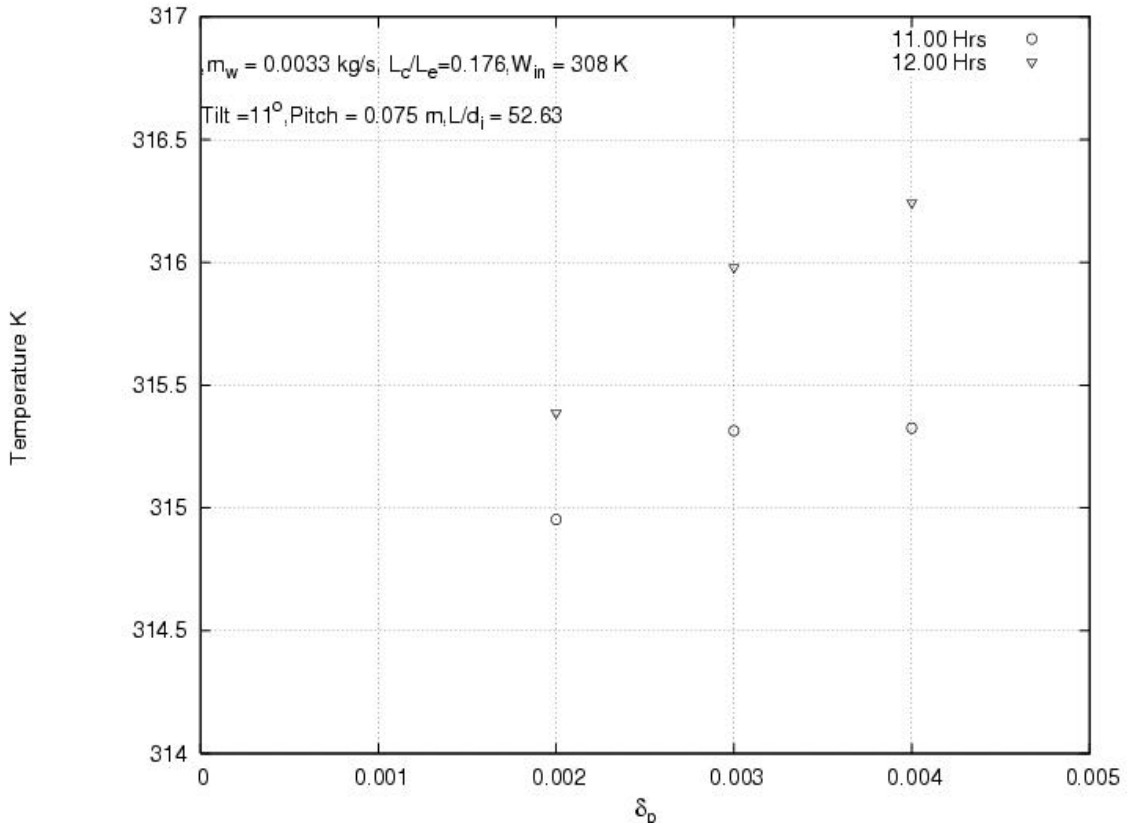

Fig. 18. Effect of δ_p on $T_{w_{out}}$.

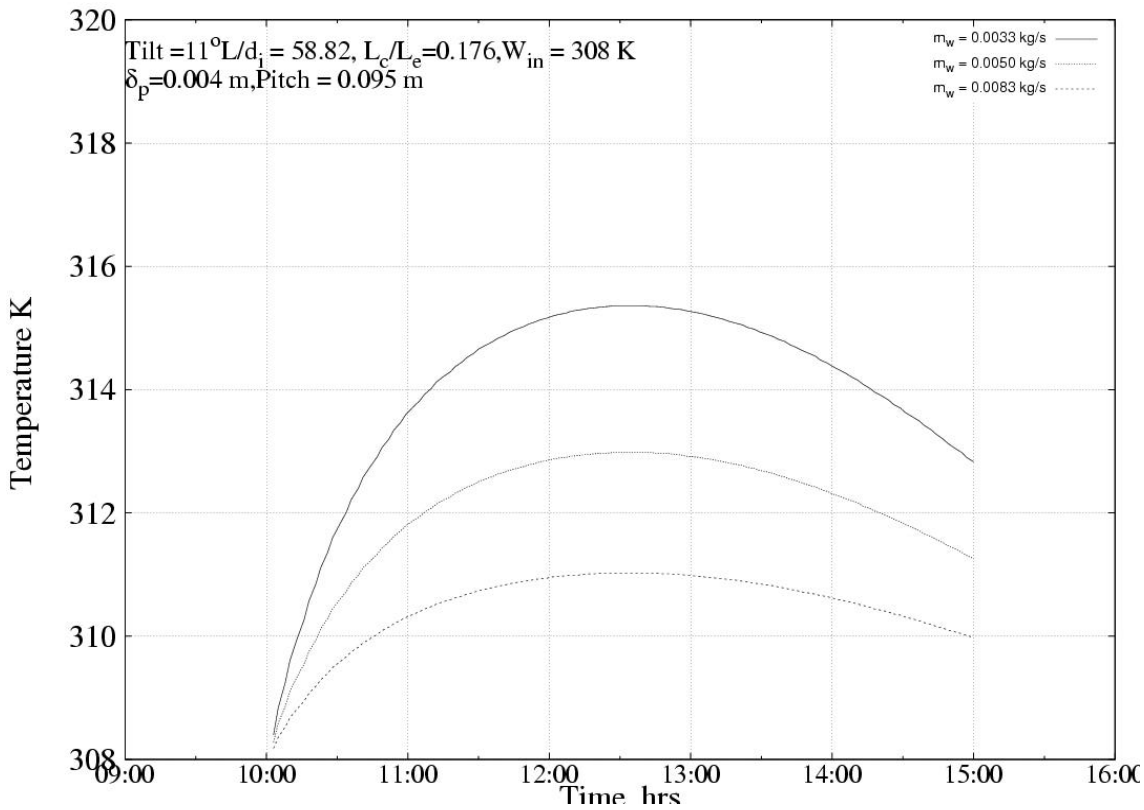

Fig. 19. Effect of m_w on $T_{w_{out}}$.

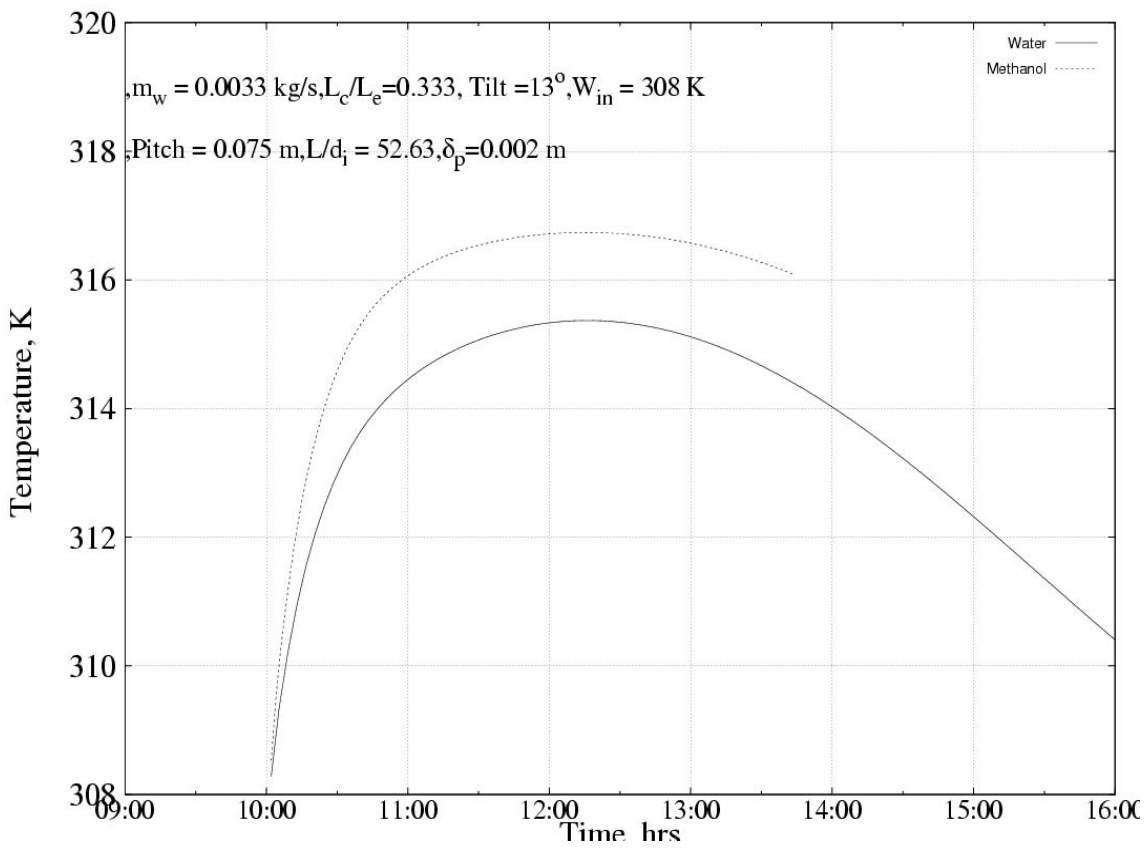

Fig. 20. Effect of working fluid on $T_{w_{out}}$.

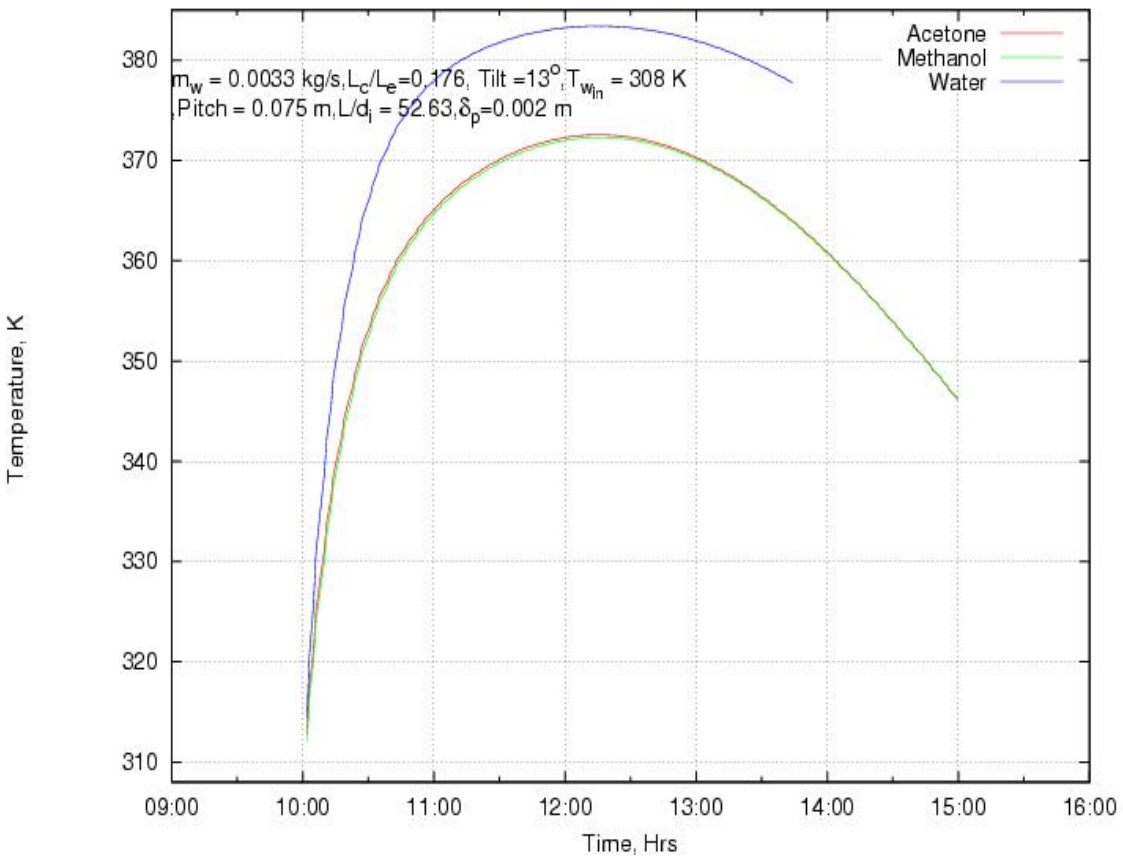

Fig. 21. Effect of working fluid on $T_{w_{out}}$

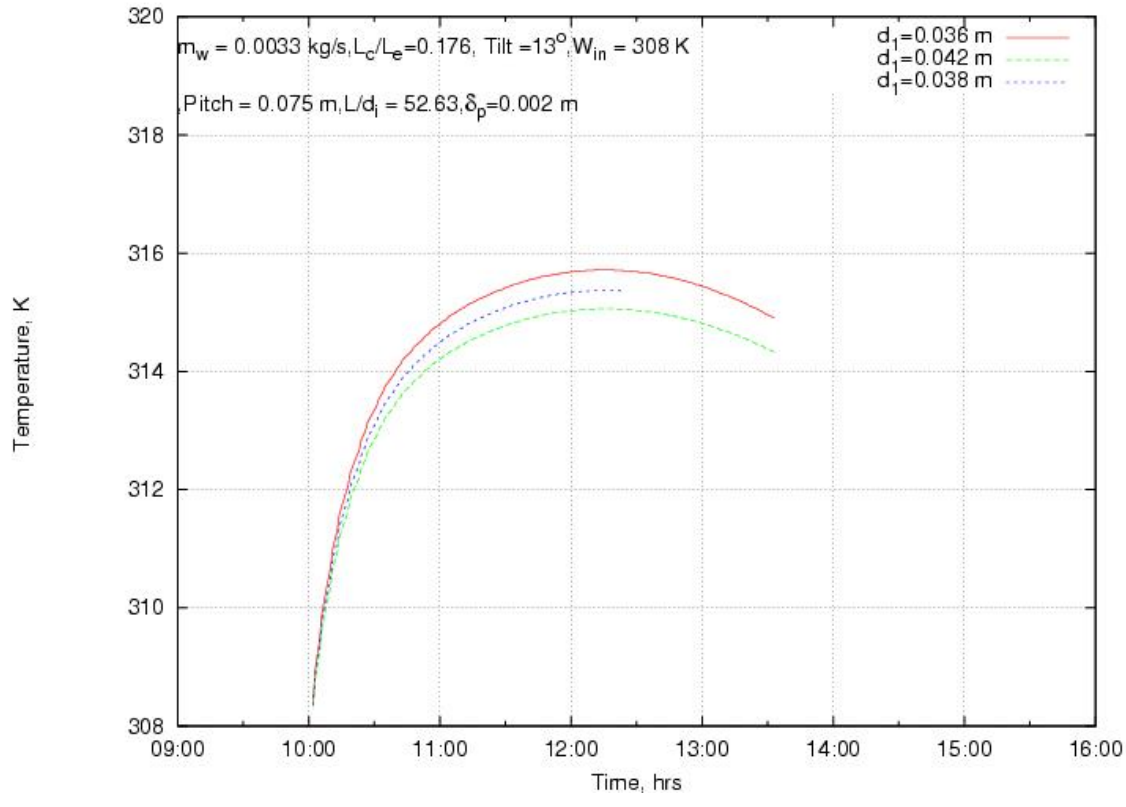

Fig. 22. Effect of heat exchanger parameter on $T_{w_{out}}$.

5. CONCLUSION

Numerical investigation on heat pipe solar collector had been carried out and the following conclusion is reported. The numerical prediction is well within the error limit on comparison with the experimental values. The effects of several parameters have been analysed in this numerical investigation and it was found that the L/d_i ratio and L_c/L_e ratio have significant effect on the performance of the collector. Between the two low boiling working fluid, methanol has found to be more effective than other fluid. It was also found that the heat exchanger dimension and thickness of the absorber also have some effect on the performance of the collector.

NOMENCLATURE

C	specific heat, J/kg K
d	diameter, m
h	heat transfer coefficient, W/m^2 K
I	Solar Intensity, W/m^2
k	thermal conductivity, W/m K
L	length, m
$\dot{m}$	mass flow rate, kg/s
P	pitch distance, m
t	time, s
T	Temperature, K
U	overall heat transfer coefficient, W/m^2 K
V^*	liquid filling ratio, dimensionless
w	absorber plate width, m
x, y	co-ordinates

Greek letters

α	absorptivity, dimensionless
δ	thickness, m
φ	porosity of wick dimensionless
μ	dynamic viscosity, N s/m^2

ρ	density, kg/m^3
τ	transmittance, dimensionless

Subscripts

a	ambient
α	sky
b	bottom
c	condenser section
ccs	wall cross-section of condenser section $_c$
cga	convection between glass cover and ambient
e	evaporator section
ecs	wall cross-section of evaporator section
eff	effective
eg	evaporator to glass cover
ex	heat exchanger
excs	heat exchanger cross section
fi	inner film heat transfer between condenser section and cooling water
fo	outer film heat transfer between water and heat exchanger
g	glass cover
i	inside
l	working fluid inside the heat pipe
o	outer
p	absorber plate
pg	plate to glass cover
rga	radiation between glass cover and sky
rpg	radiation between absorber plate and glass cover
s	saturation
t	time, total
v	vapour, vapour core
w	water, wind
w_i	inlet cooling water
w_{out}	outlet cooling water
1	inside diameter of heat exchanger
2	outside diameter of heat exchanger

REFERENCES

[1] Abogderah, M M and Ismail, K A R. 1988. Performance of a heat pipe solar collector, *Solar Energy*, 120:51 – 59.

[2] Reay D.A. 1982, Advances in Heat Pipes Technologies, edited by Pergamon Press, Oxford, UK.

[3] Al-Hindi A.R Khalifa A M and Akyurt M. 1988. Intermittent duty solar refrigerator assisted by heat pipes, *Solar and Wind Technology*5: 459 – 465.

[4] Bienert W B & Wolf D A. .Heat pipe applied to flat plate collectors, Final report COO/2604 – 76 /1

[5] Chi S W 1976 edited by James P Harnet & Thomas F Irvine JR. *Heat pipe theory and practice*, McGraw Hill, New York: 31 – 95.

[6] Chakradhar Lingamgunta, Nejat Veziroglu T. 2004. A universal relationship for estimating clear sky insolation, "*Energy Conversion and Management"*, 45: 27-52

[7] Dunn P & Reay D A 1976. *Heat pipes*, Pergamon Press, Oxford, UK: 235 - 271.

[8] Hammad M 1995. Experimental study of the performance of a solar collector cooled by heat pipes, *Energy Conversion Management* 36: 197 – 203.

[9] Hussein H M S, Mohamad M A and El-Asfouri A S 1999. Optimization of a wickless heat pipe flat plate solar collector, *Energy Conversion Management* 40: 1949–1961.

[10] Jorge Facao, Szaboics Varga and Armando C. Oliveira. 2003 Evaluation of the use of Artificial neural networks for the simulation of hybrid solar collector, In *Proceedings of first International Energy , Energy and Environmental symposium*, Turkey: 833 – 839.

[11] Kamminga W, 1986. The testing of an evacuated tubular collector with heat pipe using Fourier frequency domain, *International Journal of Heat and Mass Transfer* 29: 83 – 90.

[12] Mehmet Akurt, 1984. Development of heat pipes for solar water heaters, *Solar Energy* 32: 625 – 631.

[13] Nesreen G and Yvonne N, 1998. Experimental study of refrigerant charged solar collector, *International Journal of Energy Research* 22: 625 – 638.

[14] Schreyer J M., 1981. Residential application of refrigerant charged solar collectors, *Solar Energy* 26: 307–312.

[15] Sivaraman B and Krishna Mohan N, 2003. Experimental analysis of Condenser / Evaporator length on the performance of heat pipe solar collector, In *Proceedings of International Conference on Energy Environmental Technology for sustainable development*, MNIT, Jaipur: 417-420.

[16] Sivaraman B & Krishna Mohan N, 2005. Experimental analysis of heat pipe solar collector with different L/d_i ratio of heat pipe, Journal of Scientific & Industrial Research 64: 698- 701.

[17] Soin R S, Sangameswar Rao K, Rao D P and Rao K S, 1979. Performance of flat plate solar collector with fluid undergoing phase change, *Solar Energy* 23: 69 – 73.

[18] Soin R S, Raghuraman S and Murali V, 1987. Two phase water heater model and long term performance, *Solar Energy* 38: 105 – 112

[19] Soteris A Kalogirou, Sofia Panteliou and Argiris Dentsoras, 1999. Modelling of solar domestic water heating system using Artificial Neural Networks, *Solar Energy* 65: 335 – 342.